

# ULRR

## Performance analysis of “WBC over DVB-H” link layer

Item Type	Article
Authors	Ji, Zhanlin;Ganchev, Ivan;Ó Droma, Máirtín
Citation	EURASIP Journal on Wireless Communications and Networking;306709
Publisher	Hindawi Publishing Corporation
Download date	2026-03-11 07:01:17
Item License	<a href="https://creativecommons.org/licenses/by-nc-sa/1.0/">https://creativecommons.org/licenses/by-nc-sa/1.0/</a>
Link to Item	<a href="https://hdl.handle.net/10344/6424">https://hdl.handle.net/10344/6424</a>

## Research Article

# Performance Analysis of “WBC over DVB-H” Link Layer

Zhanlin Ji, Ivan Ganchev, and Máirtín O’Droma

*Telecommunications Research Centre, University of Limerick, Limerick, Ireland*

Correspondence should be addressed to Ivan Ganchev, [ivan.ganchev@ul.ie](mailto:ivan.ganchev@ul.ie)

Received 28 August 2009; Accepted 15 December 2009

Academic Editor: Yevgeni Koucheryavy

Copyright © 2010 Zhanlin Ji et al. This is an open access article distributed under the Creative Commons Attribution License, which permits unrestricted use, distribution, and reproduction in any medium, provided the original work is properly cited.

This paper presents two novel smart cross-layer error-control coding schemes for improving the error protection of service advertisements that are broadcast to mobile terminals on wireless billboard channels (WBCs) established over a digital video broadcast-handheld (DVB-H) infrastructure. These are the smart section erasure (SSE) and smart transport stream erasure (STSE) schemes, which are jointly executed by the link layer and service layer cross-layer algorithms. The new schemes are analysed and compared to existing schemes. The solution enables the “WBC over DVB-H” system to operate with good flexibility, and in a more reliable way and with greater throughput efficiency than the standard IP datacasting supported in DVB-H.

## 1. Introduction

Wireless billboard channels (WBCs) are novel infrastructural components of the emerging ubiquitous consumer wireless world (UCWW) [1–5]. UCWW is particularly matched to maximizing the efficient and economic use of the massive, and ever-growing, range of wireless communications interfaces, access networks’ communications services and teleservices. It is particularly in harmony with the thrust to realize the user-driven always best-connected and best-served (ABC&S) communications paradigm [6, 7]. In it, the mobile user (MU) acts as a consumer and is identified by a personal, network-independent and location-independent, IPv6 address. The consumer is not constrained to any particular access network provider (ANP) and may use any available teleservice through any available access network that best matches consumer’s needs at any time or place. For the use of services an MU pays through a trusted third-party authentication, authorization, and accounting service provider (3P-AAA-SP). The service providers (xSPs)—ANPs, value-added service providers (VASPs), and teleservice providers (TSPs)—can benefit from simplicity of having a single business agreement with 3P-AAA-SP and from the easier entry in the wireless communications market in order to succeed, and so forth.

In UCWW maximizing the volume of consumer wireless transactions, and not the number of subscriber contracts,

is the primary business driver for service providers. The newly conceived WBC infrastructural component of UCWW aims to satisfy the requirement in this environment of facilitating the service providers “pushing” advertisements and information about their service offerings to potential consumers. Taking into account the potentially large number of services already available, efficient and easy-to-implement mechanisms for services’ advertisement, discovery, and association (ADA), adapted to the terminal capabilities, user preferences, and user location, need to be developed for WBC.

A number of carrier technologies are suitable to carry the WBC dataset, for example, the digital audio broadcast (DAB), digital multimedia broadcasting (DMB), digital radio mondiale (DRM), digital video broadcast-handheld (DVB-H), multimedia broadcast/multicast service (MBMS), satellite DMB (S-DMB), digital audio radio satellite, and so forth. Among these technologies the DVB-H is an attractive solution due to its full support for IP datacasting (IPDC). The IPDC over DVB-H [8, 9] is a new European Telecommunications Standards Institute’s (ETSI) standard which enables effective distribution of digital content to mass audiences. As commercial DVB-H services have already been rolled out, the market prospect of DVB-H devices seems very bright [10].

The layered architecture of the designed “WBC over DVB-H” system is shown in Figure 1. The error protection

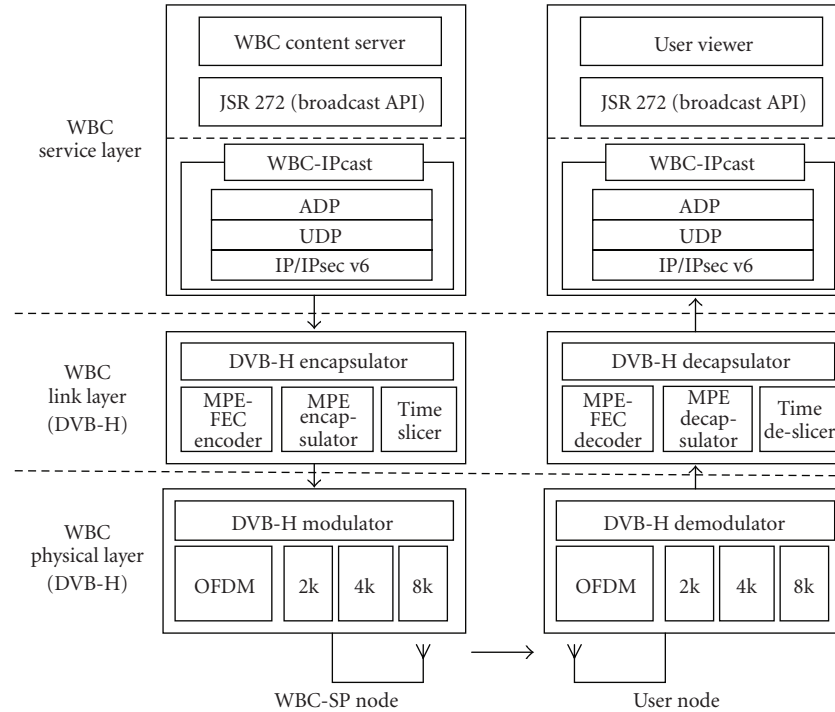


FIGURE 1: The “WBC over DVB-H” layered architecture.

of service advertisements in WBC is an important issue since even a single bit error (in an unprotected message) may result in failure to decode a particular WBC data segment [11]. A section erasure (SE) decoding algorithm based on a cyclic redundancy check (CRC-32) scheme is recommended in the standard ETSI’s DVB-H implementation guidelines [8]. However, for certain applications the potential throughput efficiency can be impeded enough since the multiprotocol encapsulation-forward error correction (MPE-FEC) frame may be marked as incorrect even if it happens that some self-contained parts of it are error-free. In [12, 13], a transport stream erasure (TSE) decoding scheme and two hierarchical erasure-plus-error Reed-Solomon (RS) decoding schemes were proposed in the link layer to improve reliability. The hierarchical decoding schemes in [13] lead to complex hardware design of the DVB-H link layer. In this paper, two new smart cross-layer encoding and decoding schemes—smart section erasure (SSE) and smart TSE (STSE)—for improving the reliability and throughput efficiency of WBC datacasting are proposed, analyzed, and compared to the existing schemes.

The rest of the paper is organized as follows. Section 2 provides an overview of the “WBC over DVB-H” link layer and describes the link layer’s encapsulation, encoding, decapsulation, and decoding schemes. Section 3 explains the two new smart cross-layer encoding and decoding schemes. Section 4 focuses on the theoretical analysis, and Section 5 on a simulation to obtain performance results for “WBC over DVB-H” in a Rayleigh fading channel environment. Section 6 summarizes the conclusions.

## 2. “WBC over DVB-H” Link Layer

In 2004, the ETSI ratified the standard of DVB-H, which is an amendment of the digital video broadcasting-terrestrial (DVB-T) standard [14] and takes into account the specific properties of a typical portable mobile terminal (MT), such as limited battery-life, various signal environments, Doppler effect, propagation loss of indoor reception, limited antenna gain, and poor weather conditions. To enable an IPDC function, two new features were introduced into the DVB-H link layer, namely, time-slicing and MPE-FEC.

This is the platform for which we have designed a “WBC over DVB-H” implementation. In this, the WBC link layer acts as a bridge between the service layer (SL) and physical layer (PHY) for transforming the IP packets into transport stream (TS) packets, adding appropriate error protection and so forth, and performing the inverse operations at the receiver. An example of the three-layer encapsulation structure of “WBC over DVB-H” protocol data units (PDUs) is presented in Figure 2.

**2.1. Time-Slicing.** In DVB-T, all channels are multiplexed by means of an orthogonal frequency division multiplexing (OFDM) and broadcast in parallel. To receive data from a channel, MTs need to stay in active mode all the time, with no allowance made for the need to conserve battery power in the mobile unit. Responding to the normal MT requirement of efficient use of battery energy—maximizing battery inter-charge life—a time-slicing mechanism is used in DVB-H for arranging the data broadcasting in a burst mode.

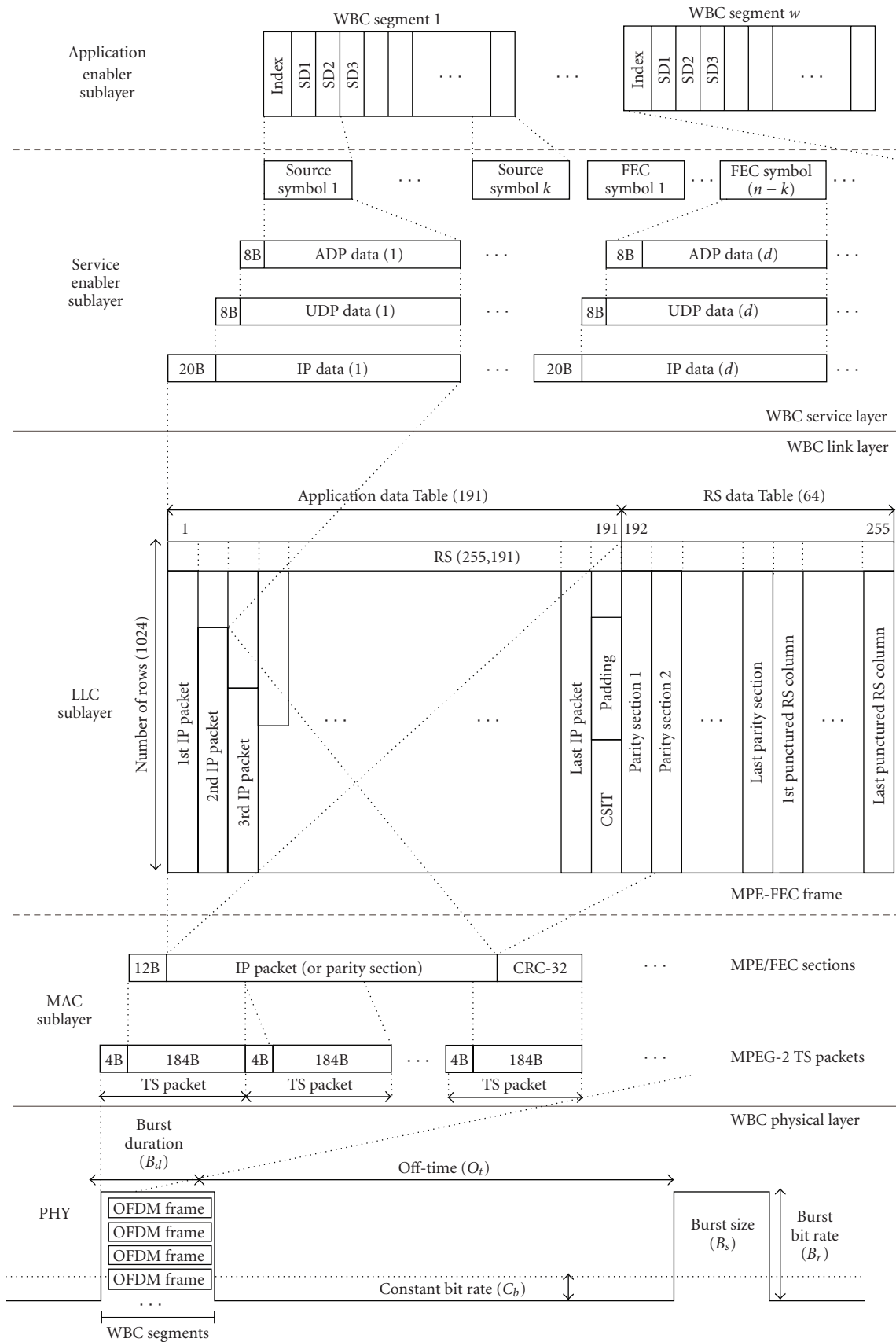


FIGURE 2: The "WBC over DVB-H" PDUs' encapsulation over the three main WBC layers.

With this mechanism MT remains most of the time in a sleep mode and becomes active only when a *target burst* is broadcast on air. A target burst is one likely to contain service description data of interest to the mobile user, as determined by his/her profile stored on the MT. The off-time between each burst is denoted by ETSI as  $O_t$  (seconds) and the relative minimum time to the beginning of the next burst from the start of the present MPE (or MPE-FEC) section being received is  $\delta$  [8]. To successfully receive a data burst, MT should become active a little bit before the scheduled arrival of the target burst. This is to allow for variation in the actual arrival time from the scheduled arrival time due to the  $\delta$ -*t jitter*  $D_j$  (10 ms by default) and the *synchronization-time*  $S_t$  (250 ms by default) [8].

The WBC burst duration is defined in [8] as

$$B_d = \frac{B_s}{B_r \times (1 - \text{overhead})}, \quad (1)$$

where  $B_s$  is the burst size (bits),  $B_r$  is the burst bit rate (bits per second), and *overhead* is the overhead fraction resulting from the TS packet and section headers.

By comparison with a constant bit rate (CBR) channel, the power saving when employing the time-slicing mechanism could be calculated as in [8]:

$$1 - \frac{(B_d + S_t + 0.75 \times D_j) \times C_b \times (1 - \text{overhead})}{B_s}, \quad (2)$$

where  $C_b$  denotes the CBR (bits per second).

**2.2. Multiprotocol Encapsulation-Forward Error Correction (MPE-FEC).** MPE-FEC is introduced in DVB-H to compensating for the performance degradations in wireless fading channels. The MPE-FEC frame is constructed as a table consisting of 255 columns and a number of rows (256, 512, 768, or 1024; [8] and Figure 2). Each cell in the table contains one byte. The 255 columns are divided in two parts: from 1st to 191st column—an application data table (ADT), and from 192nd to 255th column—a RS data table (RSDT). The IP packets are installed into the ADT column-wise, one by one. An RS code is used on each row of ADT for improving the link-layer error protection. Some parity columns are punctured to achieve different MPE-FEC code rates. Usually one DVB-H burst contains only one MPE-FEC frame. Each DVB-H burst carries a number of WBC segments.

**2.3. Encapsulation and Encoding Algorithms.** On the WBC service provider's (WBC-SP) side, the IP packets are cached on transition from the WBC service layer to the WBC logical link control (LLC) sublayer of the DVB-H link layer. When the number of IP packets in the cache becomes sufficient to fill the ADT, the IP packets are encapsulated into ADT in column-wise fashion, one by one. Then an RS (255,191) encoder runs on each row of ADT to generate 64 RS parity bytes, which are inserted into the corresponding FEC row. After the MPE-FEC frame is fully constructed, at

TABLE 1: Parameters of MPE/FEC and TS Headers.

MPE/FEC Header	Bits	TS Header	Bits
table_id	8	sync_byte	8
section_syntax_indicator	1	transport_error_indicator	1
private_indicator	1	payload_start	1
reserved	2	transport_priority	1
section_length	12	packet_identifier	13
payload_scrambling_control	2	trans_scrambling_control	2
address_scrambling_control	2	adaption_field_control	2
llc_snap_flag	1	ts_counter	1
current_next_indicator	1	ts_counter (con.)	1
reserved	2	ts_counter (con.)	2
section_number	8		

the medium access control (MAC) sublayer, each IP packet in ADT and each column of RSDT are extracted for adding a MAC overhead, that is, 12B MPE/FEC header and 4B CRC-32 trailer (Figure 2). The resultant MPE/FEC data units are segmented into an MPEG-2 transport stream (TS) for broadcasting over the channel. Each TS packet consists of 4B header and 184B payload, and is encoded at the physical layer by using an RS (204, 188) code for further error protection.

Compared with the standard DVB-H link layer, our “WBC over DVB-H” link layer uses an additional 8B smart correct segment index table (CSIT), which is inserted at the end of the last WBC segment's padding area to help the decoder operate in an efficient way. CSIT includes the size of the erasure info table (EIT), used to store the decoding information, the number of WBC segments in one MPE-FEC frame, the advertisements delivery protocol's (ADP) parameters, and so forth.

A description of the first 40 bits of the MPE/FEC header and the 32 bits of the TS header is provided in Table 1.

**2.4. Decapsulation and Decoding Algorithms.** The encapsulation and encoding schemes are stated in the DVB-H standard [8]. The design of the decoding method, however, is open.

In [8], an SE decoding scheme is suggested as follows. At the *MAC sublayer*, the MPE/FEC section is first generated from the received TS packets, and a CRC-32 code verifies it. If verification is successful, the MPE/FEC section is marked as “reliable”; otherwise it is marked for “erasure”. Then the IP packet/parity section is extracted and together with the CRC verification result is sent to the LLC sublayer. At the *LLC sublayer*, the ADT/RSDT columns are generated from the received MPE/FEC sections one by one. The corresponding bits of EIT are filled with “0s” for “reliable” packets/columns and with “1s” for those marked for “erasure”. When the MPE-FEC frame is fully reconstructed, the decoding algorithm checks the number of “1s” in the ADT part of EIT and the number of “0s” in the RSDT part of EIT. For any row, if the number of “1s” in the ADT part is smaller than the number of “0s” in the RSDT part, the MPE-FEC frame can be decoded with the RS algorithm; otherwise the decoding will fail.

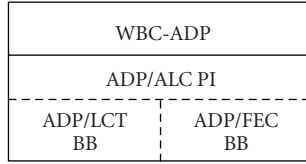


FIGURE 3: The ADP building block structure.

To improve error protection, in [13] a TSE scheme is suggested. Compared with SE, at the MAC sublayer the TSE MPE/FEC section decoding does not depend on the CRC scheme. It uses a bit indicator—*transport\_error\_indicator* (TEI), located in the TS header—to identify whether the TS packet was or was not decoded successfully with the RS(204,188) at the physical layer. If TEI = 0, the decoding was successful. If TEI = 1, the decoding failed (this includes *packet\_IDentifier* (PID) decoding failure and payload decoding failure). At the LLC sublayer, the corresponding TS packet position of EIT is filled with “0” or “1”, and the decoding scheme is the same as in SE. As the TS payload is smaller than the MPE/FEC section’s payload, the TSE scheme outperforms the SE scheme [13].

### 3. Smart Cross-Layer Encoding and Decoding Algorithms for “WBC over DVB-H”

**3.1. Advertisements Delivery Protocol (ADP).** The ADP encoding and decoding are basic elements used in the smart cross-layer encoding and decoding algorithms for “WBC over DVB-H” link layer [3, 15]. The core ADP elements include building blocks (BBs) and protocol instantiation (PI). Two modified BBs—layered coding transport (LCT) and FEC—and one modified asynchronous layered coding (ALC) PI were developed for ADP. Figure 3 depicts the ADP building block structure.

As the WBC segment is small in size, based on previous studies, the one-dimensional small-block RS codes are particularly well suited for ADP due to their characteristics, for example, good performance in correcting wireless burst errors, no “coupon collector problem”, and so forth, [15].

The ADP decoding scheme includes packet erasure decoding (PED) and packet erasure plus byte error decoding (PE+BED) schemes.

Figure 4 shows an example of the PED process. An 8kB WBC segment is first divided into 8 equal-size IP packets, which are then encoded by an RS ( $n, k$ ) algorithm (where  $n = 10$ , is the number of encoding symbols per WBC segment;  $k = 8$  is the number of source symbols per WBC segment). This way the receiver can recover a WBC segment from any 8 (out of 10) encoding symbols received without errors.

The PE+BED scheme is explained in detail in [16].

**3.2. Link Layer.** Being not designed for WBCs with their specific characteristics in mind, the SE and TSE decoding processes are not efficient for direct use in WBCs. As one DVB-H burst (MPE-FEC frame) usually contains several

WBC segments, even a single byte error in the MPE-FEC frame may cause a decoding failure. To improve the error protection in WBCs, the CSIT used by ADP for cross-layer decoding was developed.

The decapsulation process of the WBC smart cross-layer decoding is similar to that described in Joki and Paavola [13]; that is, it maps into a smart SE (SSE) and a smart TSE (STSE) schemes.

The WBC smart decoding process, however, is different as per algorithm.

- (1) Try to decode each row  $j$  of the MPE-FEC frame. In case of failure, mark the undecoded rows and go to step 2.
- (2) Initialize CSIT. Execute the following Algorithm 1 ( $w$  denotes the number of WBC segments in an MPE-FEC frame,  $x$  denotes the number of column(s) occupied by each IP packet).

Comparing with SE and TSE decoding schemes, the new WBC smart cross-layer decoding schemes provide better error protection. On the other hand, due to the fact that the WBC smart decoding works with the ADP protocol, the time complexity is increased from  $O(k \times l \times x)$  to  $O(k \times (n - k + l + l \times x))$ , where  $l$  is the number of lost packets. This, however, is acceptable because the complexity increases linearly.

The functional model of the “WBC over DVB-H” link-layer decoder is depicted in Figure 5.

**3.3. Service Layer.** To further improve the error protection, the PE+BED algorithm runs at the bottom of the service layer.

Figure 6 shows the WBC segment error rate (SER) as a function of the IP packet error rate (IPER) for PED and PE+BED schemes in memoryless channel, where  $n = 10$ ,  $k = 8$ , and the IP packet length is 1024B. The results show that the PE+BED scheme outperforms the PED scheme.

On the MU side, the decapsulation and decoding scheme is selected automatically by MT based on the MT’s composite capability/preference profile (CC/PP) [17]. MTs with very limited capabilities should select the SE decoding algorithm, whereas MTs with reasonable computing capabilities should select the STSE decoding algorithm.

## 4. IPER and SER Analysis

IPER and SER are important criteria for measuring the decoding performance for “WBC over DVB-H” link layer. In this section, the theoretical analysis of IPER and SER is performed by means of a one-state loss model (i.e., the bit/byte error rate follows a uniform distribution).

Table 2 lists the notations used in this section.

To simplify the analysis, similarly to [12] the size of the IP packet is set to  $N = 535$  bytes (B) (i.e., close enough to the standard value for  $N$  of 512). Each MPE-FEC column generates 3 TS packets with payloads of 171B, 184B, and 180B, respectively. The first TS packet includes the 12B MPE/FEC section’s header and the 1B section start indicator,

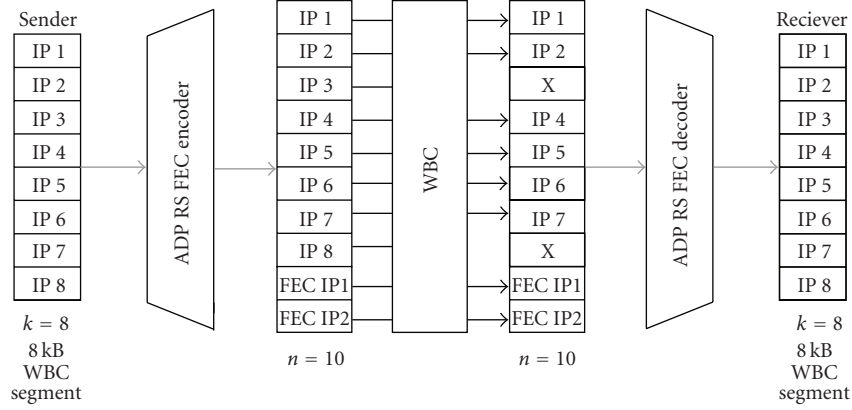


FIGURE 4: A graphical representation of the ADP packet erasure encoding/decoding process.

**in the link layer:**

```

for i = 1 to w
  if there are "1s" in corresponding EIT columns,
    then
      (a) extract  $i \times x \times n$  IP packets from the MPE-FEC
            frame, and
      (b) decode with ADP in packet erasure mode.
            if a WBC segment is decoded successfully,
              then
                (a) encode the recovered WBC segment
                      into IP datagrams with ADP packet
                      erasure scheme, and
                (b) fix the corresponding MPE-FEC cells
                      and EIT table.
                (c) try to run the RS algorithm on
                      the MPE-FEC frame.
              end if
            end if
          end if
        i = i + 1
      end for.
    if EIT contains errors,
      for i = 1 to w
        if  $IP(\text{good}) < k$ , fill the ADP header reserved area (r)
          with "1".
        endif
      endfor
    endif
    forward IP packets to the service layer.
  
```

ALGORITHM 1

whereas the last TS packet includes the corresponding 4B CRC-32 code.

4.1. *Smart Section Erasure (SSE)*. In SSE, the probability  $p_c$  of a MPE column error occurring is

$$p_c = 1 - (1 - p_b)^N, \quad \text{where } p_b = 1 - (1 - p)^8. \quad (3)$$

TABLE 2: Parameter definitions.

$w$	Total number of WBC segments in MPE-FEC frame
$d$	Number of RSDT columns in MPE-FEC frame
$p$	Bit error probability in binary symmetric channel (BSC)
$p_b$	Byte error probability in BSC
$p_c$	MPE column error probability in BSC
$p_t$	TS packet error probability in BSC
$N$	Number of rows of MPE-FEC frame
$M$	Number of columns of MPE-FEC frame being filled

As  $w$  WBC segments are installed in one MPE-FEC frame, then

$$M = w \times n + d. \quad (4)$$

With the SE decoding scheme, in order to reconstruct the MPE-FEC frame, at least  $w \times n$  columns (out of  $M$ ) must be received with no errors. Then the MPE-FEC error rate (MFER) can be obtained as

$$\text{MFER} = 1 - \sum_{i=w \times n}^{j=M} C_j^i (1 - p_c)^i p_c^{j-i}. \quad (5)$$

The IPER after the SE decoding can be obtained as

$$\text{IPER} = 1 - (1 - \text{MFER})^{1/M}. \quad (6)$$

Then the corresponding SER can be obtained as

$$\text{SER} = 1 - (1 - \text{IPER})^k. \quad (7)$$

After executing the smart cross-layer decoding algorithm (ADP PED) in the LLC sublayer, the link layer SER, IPER, and the corresponding byte error rate can be obtained, respectively, as

$$\text{SER}_{\text{LL}} = 1 - \sum_{i=k}^{j=n} C_j^i (1 - \text{IPER})^i \text{IPER}^{j-i}; \quad (8)$$

$$\text{IPER}_{\text{LL}} = 1 - (1 - \text{SER}_{\text{LL}})^{1/n}$$

$$p_{\text{bLL}} = 1 - (1 - \text{IPER}_{\text{LL}})^{1/N}.$$

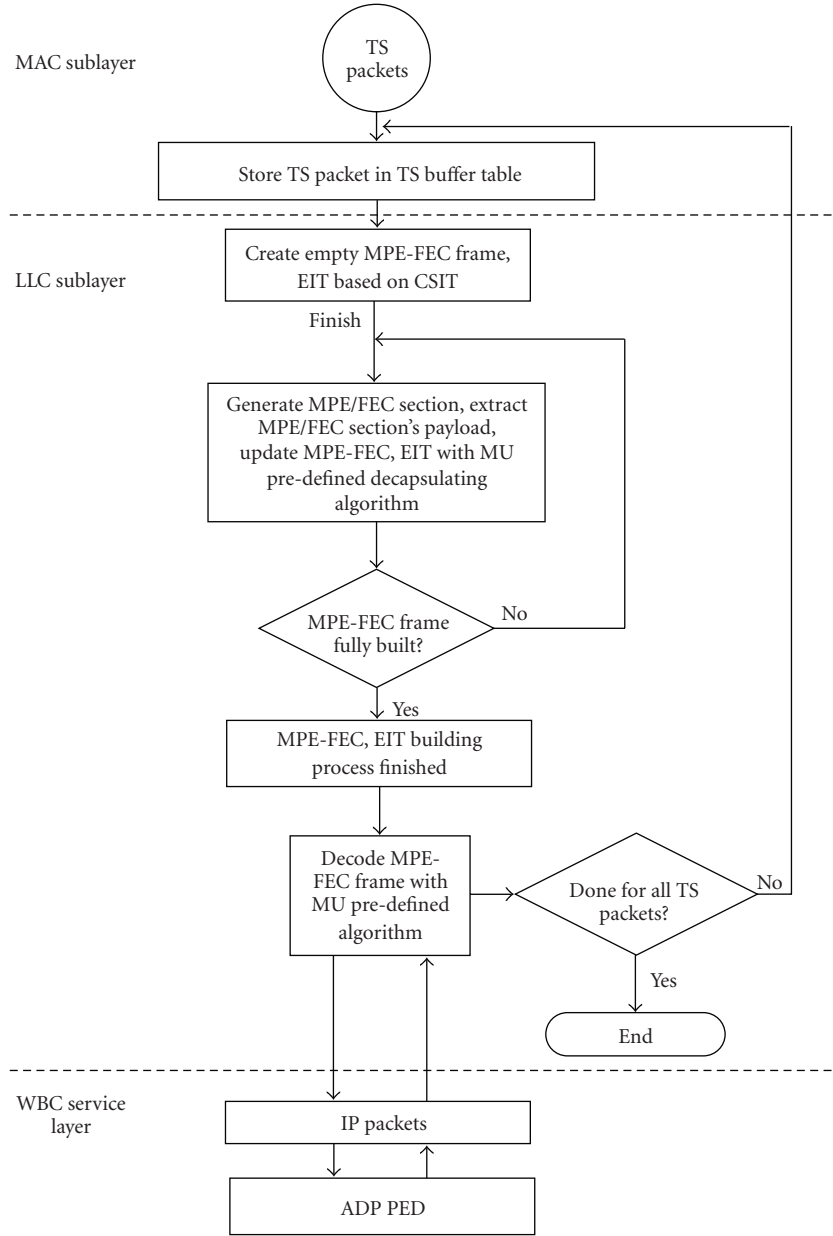


FIGURE 5: The “WBC over DVB-H” link-layer decoder’s functional model.

In the service layer, an ADP PE+BED algorithm is run if the received WBC segment contains errors. After completing the decoding process at the service layer, the service layer (SL) byte error rate can be obtained as

$$p_{bSL} = 1 - \sum_{i=k+(n-k)/2}^{j=n} C_j^i (1 - p_{bLL})^i p_{bLL}^{j-i}. \quad (9)$$

Then the corresponding IPER is

$$\text{IPER}_{SL} = 1 - (1 - p_{bSL})^N, \quad (10)$$

and the final SER can be obtained as

$$\text{SER}_{SL} = 1 - \sum_{i=k}^{j=n} C_j^i (1 - \text{IPER}_{SL})^i \text{IPER}_{SL}^{j-i}. \quad (11)$$

**4.2. Smart Transport Steam Erasure (STSE).** In STSE, considering that each TS packet contains 188 bytes, the probability  $p_t$  is

$$p_t = 1 - (1 - p_b)^{188}. \quad (12)$$

With the SE decoding scheme, in order to reconstruct the MPE-FEC frame, at least  $w \times n$  TS packets must be received with no errors in the first 171 rows, next 184 rows, and

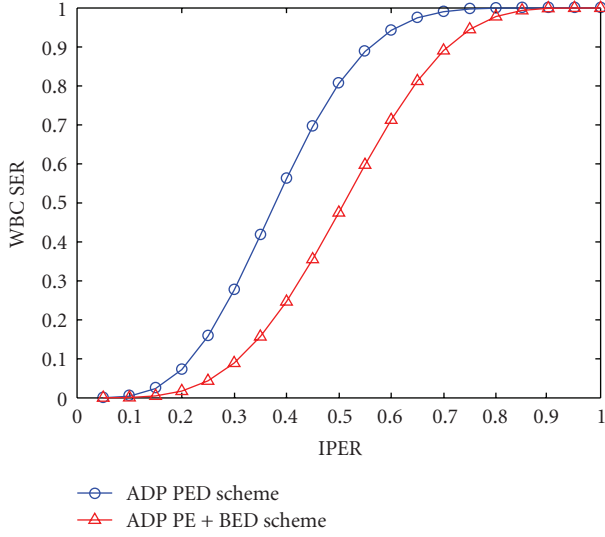


FIGURE 6: WBC SER as a function of IPER for ADP PED and for ADP PE+BED.

in the final 180 rows, respectively. Then the MFER can be obtained as

$$\text{MFER} = 1 - \left[ \sum_{i=w \times n}^{j=M} C_j^i (1 - p_t)^i p_t^{j-i} \right]^3. \quad (13)$$

The TS packet error rate (TSPER) after the SE decoding can be obtained as

$$\text{TSPER} = 1 - \left[ \sum_{i=w \times n}^{j=M} C_j^i (1 - p_t)^i p_t^{j-i} \right]^{1/M}. \quad (14)$$

Then IPER and corresponding SER can be obtained as

$$\begin{aligned} \text{IPER} &= 1 - (1 - \text{TSPER})^3; \\ \text{SER} &= 1 - (1 - \text{TSPER})^{3k}. \end{aligned} \quad (15)$$

After running the smart cross-layer decoding algorithm (ADP PED) on top of the link layer, SER, TSPER, IPER, and the corresponding byte error rate can be obtained as

$$\begin{aligned} \text{SER}_{\text{LL}} &= 1 - \left[ \sum_{i=k}^{j=n} C_j^i (1 - \text{TSPER})^i \text{TSPER}^{j-i} \right]^3; \\ \text{TSPER}_{\text{LL}} &= 1 - \left[ \sum_{i=k}^{j=n} C_j^i (1 - \text{TSPER})^i \text{TSPER}^{j-i} \right]^{1/n}; \\ \text{IPER}_{\text{LL}} &= 1 - (1 - \text{TSPER}_{\text{LL}})^3; \\ p_{\text{bSL}} &= 1 - (1 - \text{TSPER}_{\text{SE}})^{1/188}. \end{aligned} \quad (16)$$

In the service layer, after completing the decoding process (PE+BED), the byte error rate is the same as in (9), and the corresponding TSPER is:

$$\text{TSPER}_{\text{SL}} = 1 - (1 - p_{\text{bSL}})^{188}. \quad (17)$$

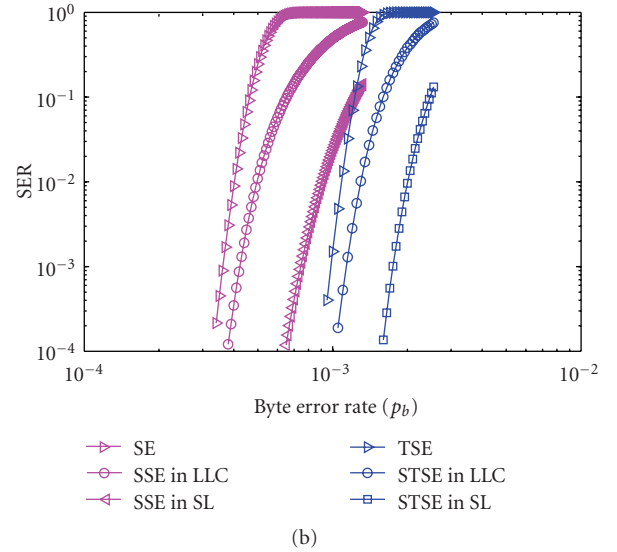
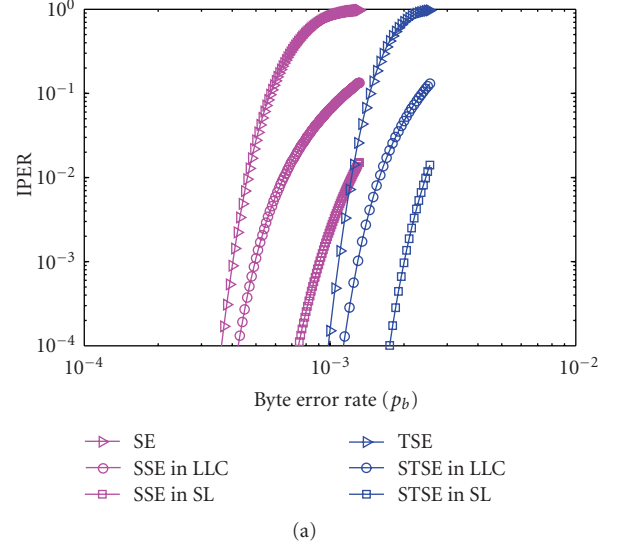


FIGURE 7: The comparison of decoding schemes on (a) IPER and (b) SER (In both figures the left three graphs correspond to the SE and two SSE results).

The final IPER and SER can be obtained as:

$$\begin{aligned} \text{IPER}_{\text{SL}} &= 1 - (1 - \text{TSPER}_{\text{SL}})^3; \\ \text{SER}_{\text{SL}} &= 1 - \left[ \sum_{i=k}^{j=n} C_j^i (1 - \text{TSPER}_{\text{SL}})^i \text{TSPER}_{\text{SL}}^{j-i} \right]^3. \end{aligned} \quad (18)$$

**4.3. Comparison of Decoding Schemes.** Figure 7 illustrates IPER and SER as a function of the byte error rate ( $p_b$ ) for  $n = 10$  and  $k = 8$ .

The analytical results show that the CRC-based decoding schemes (SE, SSE) are not better than the TS-based schemes (TSE, STSE) because the TS packet is shorter than the MPE/FEC section and thus more efficient for decoding. The smart cross-layer decoding schemes (SSE, STSE) are better than the ordinary decoding schemes (SE, TSE) because

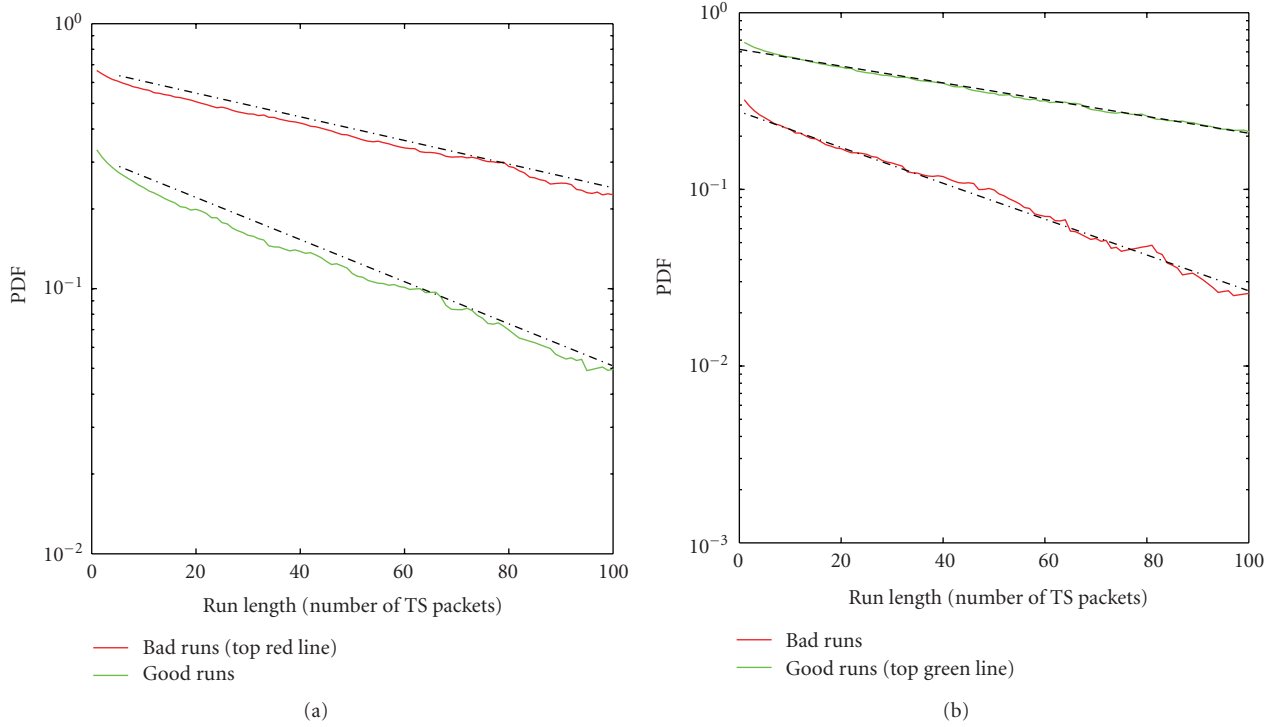


FIGURE 8: The observed probability distributions of good runs and bad runs in “WBC over DVB-H” with SNR of (a) 12 dB and (b) 15 dB. (PHY parameters: 16-QAM, CR = 1/2, 4K OFDM, GI = 1/4; WBC is assumed by Rayleigh distributed with AWGN).

the number of erasure/error columns can be corrected by ADP PED at the LLC sublayer and by PE+BED at the service layer.

## 5. Simulation Analysis of “WBC over DVB-H” Link Layer in Rayleigh Fading Channel

**5.1. Two-State Run Length Model (2SRL).** Previous studies have shown that errors in wireless channels occur in burst mode due to the multipath propagation [18–20]. In [21], a finite-state Markov model (FSMM) to represent Rayleigh fading channels in noninterleaving coding systems is introduced. In [12], a finite-state run length model for simulating the TS packet error behavior in a multipath channel environment is presented, but the model’s parameters are obtained by unbiased estimators. In [22], a two-state run length model (2SRL) for analyzing the throughput in fading channels is proposed. However, the details of the fading channel and the manner of obtaining the parameters of the model are not explained. Despite the fact that the Rayleigh fading channel with a central chi-square distribution is known to be a flexible model that provides a definable number of degrees of freedom to experimental fading channel measurements for outdoor environments [23], there are very few studies for 2SRL over a central chi-square distribution Rayleigh channel. This subsection will focus on the received signal envelope having a central chi-square distribution and will use 2SRL to analyze the physical-layer TS packets outputting behavior.

The 2SRL model was developed from the two-state Markov model (2SMM) [22]. The difference is that 2SMM is concerned with the state transition probability, whereas 2SRL is concerned with the run-length probability. There are two probability distribution functions (PDFs) in 2SRL used for statistical analysis: a good run length probability distribution  $f_g(m)$  and a bad run length probability distribution  $f_b(m)$ . With these two PDFs, the TS packets good/bad outputting can be easily generated. Figure 8 shows both PDFs for different average values of the signal-to-noise ratio (SNR), namely, 12 dB and 15 dB. The channel is assumed to be Rayleigh with additive white Gaussian noise (AWGN). The results demonstrate that by using basic curve fitting techniques (CFT), each PDF (in logarithmic scale) can be approximated as a linear function (dash line). Figure 8 also demonstrates that  $f_g(m)$  and  $f_b(m)$  can be approximated by a single geometric distribution function. Thus in “WBC over DVB-H”, 2SMM is used to approximate 2SRL.

The 2SMM model transition matrix is defined in [22] as

$$\Pi = \begin{pmatrix} 1-b & b \\ g & 1-g \end{pmatrix}, \quad (19)$$

where  $b$  and  $g$  are the transition probabilities. The steady-state probability is

$$\pi_{\text{steady\_state}} = (\pi_g, \pi_b) = \left( \frac{g}{b+g}, \frac{b}{b+g} \right). \quad (20)$$

The average number of good states can be obtained as

$$\bar{X}_g = \sum_{i=0}^{\infty} (i+1)b(1-b)^i = \frac{1}{b}, \quad (21)$$

whereas the average number of bad states can be obtained as

$$\bar{X}_b = \sum_{i=0}^{\infty} (i+1)g(1-g)^i = \frac{1}{g}. \quad (22)$$

Then the run length distributions of 2SRL can be calculated by using the 2SMM parameters  $g, p_e(G), b, p_e(B)$  as follows:

$$f_g(m) = \sum_{i=0}^m [(1-p_e(G))g]^i [(1-p_e(B))b]^{m-i}; \quad (23)$$

$$f_b(m) = \sum_{i=0}^m (p_e(G)g)^i (p_e(B)b)^{m-i},$$

where  $p_e(G)$  and  $p_e(B)$  are the error probabilities in states  $G$  and  $B$ , respectively.

5.2. 2SRL Parameters in "WBC over DVB-H". The probability density function of a central chi-square distribution is defined in [23] as

$$p_R(r) = \frac{1}{2^{(n-2)/2} \sigma^n \Gamma(n/2)} r^{n-1} \exp\left(-\frac{r^2}{2\sigma^2}\right), \quad (24)$$

where  $r$  denotes the received SNR in "WBC over DVB-H" physical layer ( $r \geq 0$ );  $\sigma^2$  is the variance of the Gaussian scattering component;  $n$  denotes the number of degrees of freedom;  $\Gamma(\cdot)$  denotes the Gamma function.

To get instantaneous SNR per symbol's PDF [24],

$$\begin{aligned} p(r)dr &= f(\gamma)d\gamma, & \gamma &= \frac{r^2 T_S}{2\sigma_n^2}, \\ d\gamma &= \frac{r T_S}{\sigma_n^2} dr, & \bar{\gamma} &= \frac{\sigma^2 T_S}{\sigma_n^2}, \end{aligned} \quad (25)$$

where  $T_S$  is the symbol time,  $\sigma_n^2$  is the power spectral density (PSD) of the noise which is equal to  $N_0/2$ , and  $\bar{\gamma}$  is the average SNR per symbol.

Then PDF of SNR per symbol can be obtained as

$$\begin{aligned} f(\gamma) &= p(r) \frac{dr}{d\gamma} \\ &= \frac{(1/(2^{(n-2)/2} \sigma^n \Gamma(n/2))) r^{n-1} \exp(-r^2/(2\sigma^2))}{r T_S / \sigma_n^2} \\ &= \frac{r^{n-2}}{2^{(n-2)/2} \Gamma(n/2) \sigma^{n-2} \sigma^2 * T_S} \exp\left(-\frac{r^2}{2\sigma^2}\right) \\ &= \frac{(\gamma)^{n/2-1}}{\Gamma(n/2) \bar{\gamma}^{n/2}} \exp\left(-\frac{\gamma}{\bar{\gamma}}\right). \end{aligned} \quad (26)$$

The cumulative distribution function (CDF) of (24) is

$$\begin{aligned} F_R(r) &= \int_{-\infty}^r p_R(x) dx \\ &= \int_{-\infty}^r \frac{1}{2^{(n-2)/2} \sigma^n \Gamma(n/2)} x^{n-1} \exp\left(-\frac{x^2}{2\sigma^2}\right) dx \\ &= \frac{1}{2^{(n-2)/2} \sigma^n \Gamma(n/2)} \int_{-\infty}^r x^{n-1} \exp\left(-\frac{x^2}{2\sigma^2}\right) dx. \end{aligned} \quad (27)$$

By letting  $u = x^2/2\sigma^2, du = x dx/\sigma^2$ ,  $F_R(r)$  equals

$$\begin{aligned} F_R(r) &= \frac{1}{2^{(n-2)/2} \sigma^n \Gamma(n/2)} \int_0^{r^2/2\sigma^2} (\sqrt{u} 2\sigma^2)^{n-1} \exp(-u) \frac{\sigma^2}{\sqrt{u} 2\sigma^2} du \\ &= \frac{\Gamma(n/2, r^2/2\sigma^2)}{\Gamma(n/2)}. \end{aligned} \quad (28)$$

Since  $r = \sqrt{(\gamma 2\sigma_n^2)/T_S}$ ,  $F_R(\gamma)$  is

$$F_R(\gamma) = \frac{\Gamma(n/2, \gamma/\bar{\gamma})}{\Gamma(n/2)}, \quad (29)$$

where

$$\Gamma\left(\frac{n}{2}, \frac{\gamma}{\bar{\gamma}}\right) = \left(\frac{n}{2} - 1\right)! \exp\left(-\frac{\gamma}{\bar{\gamma}}\right) \sum_{k=0}^{(n/2)-1} \frac{1}{k!} \left(\frac{\gamma}{\bar{\gamma}}\right)^k. \quad (30)$$

Let  $f_D = \nu f_c/c$  be the maximum Doppler frequency, where  $\nu$  is the speed of movement of the user terminal,  $f_c$  is the carrier frequency, and  $c$  is the speed of light. The expected number of times per unit interval (also known as the level crossing rate) that the received signal passes downward across level  $\gamma_t$  is given in [25] as

$$N(r_t) = \int_0^{\infty} \dot{x} p(\dot{x}, r = r_t) d\dot{x}, \quad (31)$$

where  $\dot{x}$  is the time derivative of  $r$ , and  $p(\dot{x}, r)$  is the joint PDF of  $\dot{x}$  and  $r$  at  $r = r_t$ . The PDF  $p(\dot{x})$  is obtained as

$$p(\dot{x}) = \frac{1}{\sqrt{2\pi}\hat{\sigma}} \exp\left(-\frac{\dot{x}^2}{2\hat{\sigma}^2}\right). \quad (32)$$

Let  $R = X^2 = \sum_{i=1}^n x_i^2$ , then  $E[\dot{X}] = 0$ ,  $E[\dot{X}^2] = 2(\pi f_D \sigma)^2$ , thus  $\hat{\sigma}^2 = 2(\pi f_D \sigma)^2$ .

Since  $p(\dot{x})$  and  $p(r)$  are independent [25],  $N(r_t)$  could be obtained as

$$N(\gamma_t) = \frac{\sqrt{2\pi} f_D r_t^{n-1}}{(2\sigma^2)^{(n-1)/2} \Gamma(n/2)} \exp\left(-\frac{r_t^2}{2\sigma^2}\right). \quad (33)$$

Then,  $N(\gamma_t)$  is equal to:

$$N(\gamma_t) = \frac{\sqrt{2\pi} f_D (\gamma_t/\bar{\gamma})^{(n-1)/2}}{\Gamma(n/2)} \exp\left(-\frac{\gamma_t}{\bar{\gamma}}\right). \quad (34)$$

TABLE 3: PHY Testbed's Parameters.

Parameters	Value	Parameters	Value
Modulation type	16 QAM	Operational mode	4k
Convolutional code rate	1/2	OFDM FFT size	4k
Guard interval	1/4	RF	700 MHz
Carriers' number	3409	OFDM symbol transmit time ( $t_{\text{ofdm}}$ )	448 $\mu\text{s}$
Continual pilot carriers	89	Number of OFDM symbols in OFDM frame ( $n_{\text{ofdm}}$ )	68
Cyclical prefix ratio ( $cp\%$ )	25%	Number of TS packets in OFDM frame ( $n_{\text{ts}}$ )	252

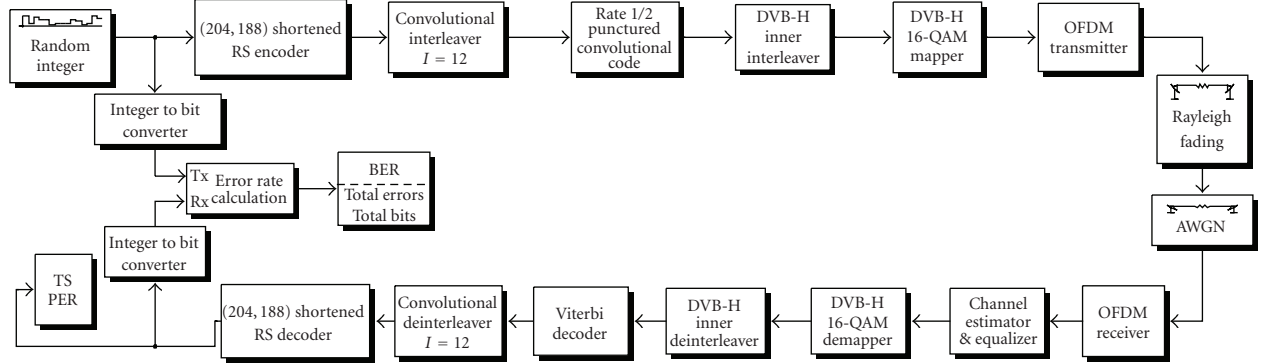


FIGURE 9: The “WBC over DVB-H” Matlab PHY Testbed.

To represent the time-varying behavior of a central chi-square fading WBC channel, the received SNR was quantized with thresholds  $\gamma_t$ . Then  $\pi_g, \pi_b$  were obtained as

$$\pi_g = \int_{\gamma_t}^{\infty} f_R(\gamma) d\gamma = F_R(\infty) - F_R(\gamma_t) = \frac{\Gamma(n/2, \gamma_t/\bar{\gamma})}{(n/2 - 1)!}; \quad (35)$$

$$\pi_b = \int_0^{\gamma_t} f_Y(\gamma) d\gamma = F_R(\gamma_t) - F_R(0) = 1 - \frac{\Gamma(n/2, \gamma_t/\bar{\gamma})}{(n/2 - 1)!}. \quad (36)$$

The transition probabilities  $g$  and  $b$  were approximated by the level crossing rate, the average number of TS packets per unit interval ( $T_p$ ), and  $\{\pi_g, \pi_b\}$ , as follows:

$$g = \frac{N(\gamma_t) T_p}{\pi_b} = \frac{\sqrt{2\pi} f_D T_p (\gamma_t/\bar{\gamma})^{(n-1)/2} \exp(-\gamma_t/\bar{\gamma})}{\Gamma(n/2) - \Gamma(n/2, \gamma_t/\bar{\gamma})}; \quad (37)$$

$$b = \frac{N(\gamma_t) T_p}{\pi_g} = \frac{\sqrt{2\pi} f_D T_p (\gamma_t/\bar{\gamma})^{(n-1)/2} \exp(-\gamma_t/\bar{\gamma})}{\Gamma(n/2, \gamma_t/\bar{\gamma})}. \quad (38)$$

Finally, the error probabilities in state  $G$  and  $B$  were obtained as described in [21]:

$$p_e(G) = \frac{\int_{\gamma_t}^{\infty} f_R(\gamma) P_e(\gamma) d\gamma}{\pi_g}; \quad (39)$$

$$p_e(B) = \frac{\int_0^{\gamma_t} f_R(\gamma) P_e(\gamma) d\gamma}{\pi_b}, \quad (40)$$

where  $P_e(\gamma)$  is the error probability for a given value  $\gamma$  in an AWGN channel. For DVB-H,  $P_e(\lambda)$  is defined as

$$P_e(\gamma) = \sum_{i=196}^{204} C_n^i [1 - p_b(\gamma)]^i p_b(\gamma)^{n-i}, \quad (41)$$

where  $p_b(\gamma)$  is the byte error rate when the received SNR is equal to  $\gamma$ .

The values of parameters  $T_p$  and  $p_b(\gamma)$  were obtained from the “WBC over DVB-H” physical layer (PHY) simulation testbed, which is described in the next subsection.

**5.3. “WBC over DVB-H” PHY Simulation Testbed.** A “WBC over DVB-H” PHY simulation testbed (Figure 9) was built using Matlab with parameters shown in Table 3.

The testbed was designed based on the ETSI-EN-300-744 standard [14]. The transmitter first generates a  $252 \times 188\text{B}$  OFDM frame dataset, which further undergoes six processing steps. During the outer coding step, a Galois field (GF) array is created with the OFDM frame. Then the array is encoded by an RS(204,188) algorithm for extra error protection at the physical layer. During the outer interleaving step, the output matrix is first reshaped to 1-row dataset; then a convolutional interleaving algorithm is used for permuting the 1-row dataset by means of an internal shift register algorithm; finally, the output is translated into a bit array by a GF 2-bit converter. During the inner convolutional step, the bit array is first encoded by the convolutional encoder and then punctured by the predefined convolutional

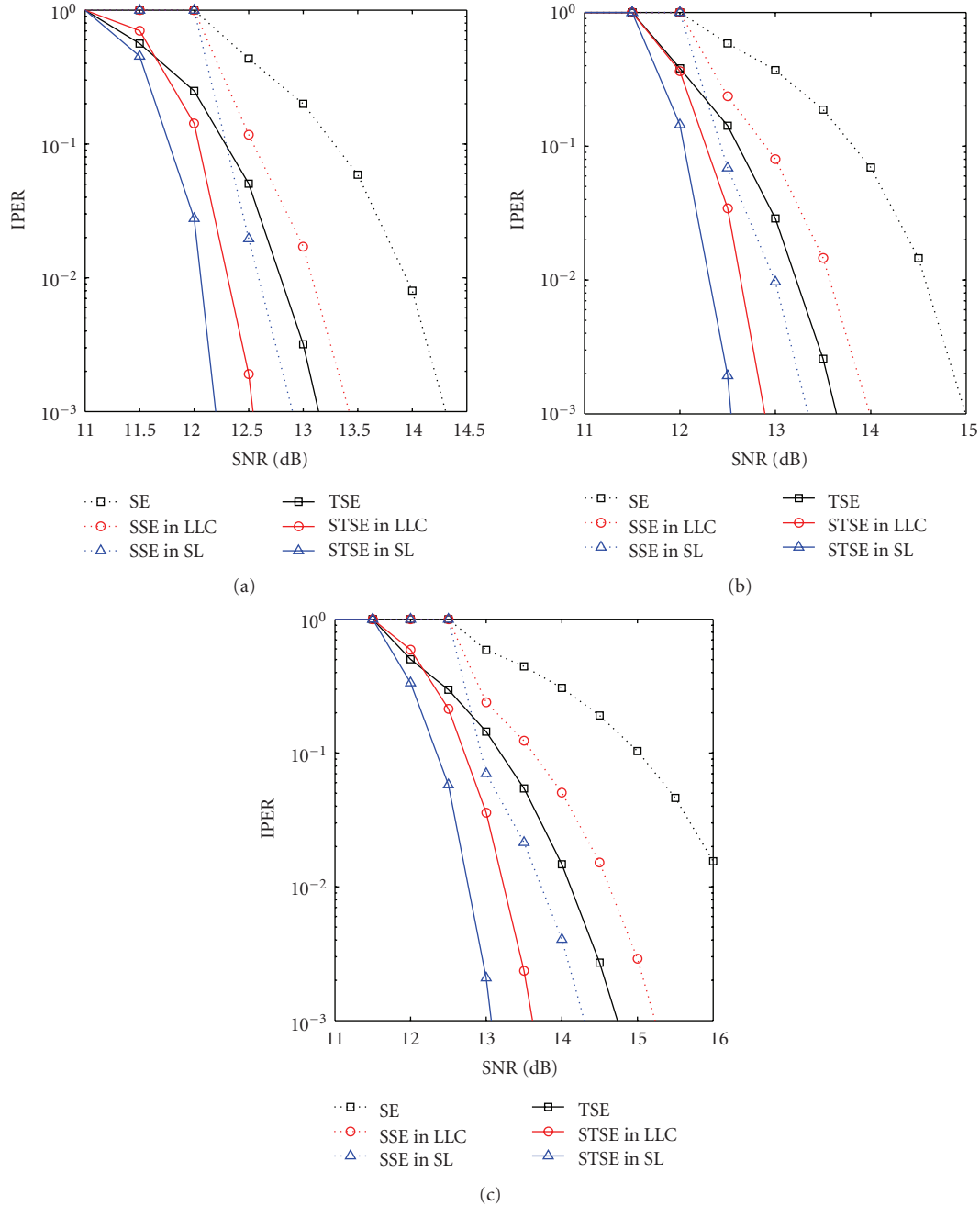


FIGURE 10: The IPER simulation results for “WBC over DVB-H”: (a)  $f_D = 10$  Hz; (b)  $f_D = 40$  Hz; (c)  $f_D = 80$  Hz.

code rate. During the interleaving step, for every 12096 bits, a block-based inner bitwise interleaving algorithm followed by a symbol interleaving algorithm is used to provide extra reliability. During the mapping and modulation steps, all data contained in one OFDM frame is modulated by a modulation algorithm. During the channel step, the output of modulation is first filtered by a chi-square fading algorithm and AWGN is added to it. The receiver processes the data in reversed order.

With the physical layer parameters obtained from the testbed, the average number of packets per unit interval ( $T_p$ ) can be calculated as follows

$$T_p = \frac{t_{\text{ofdm}} \times n_{\text{ofdm}} \times (1 + cp\%)}{n_{ts}}. \quad (42)$$

**5.4. Simulation Results.** With the calculated values of 2SMM parameters, the run length probability distributions  $f_g(m)$  and  $f_b(m)$  of 2SRL can be calculated. Thus the 2SRL can easily represent the output behavior (good/bad TS packet output) for the “WBC over DVB-H” physical layer (i.e., “0” represents a good TS packet output and “1” represents a bad TS packet output). This way the data processing at the “WBC over DVB-H” link layer is reduced and the decoding algorithms running time is acceptable.

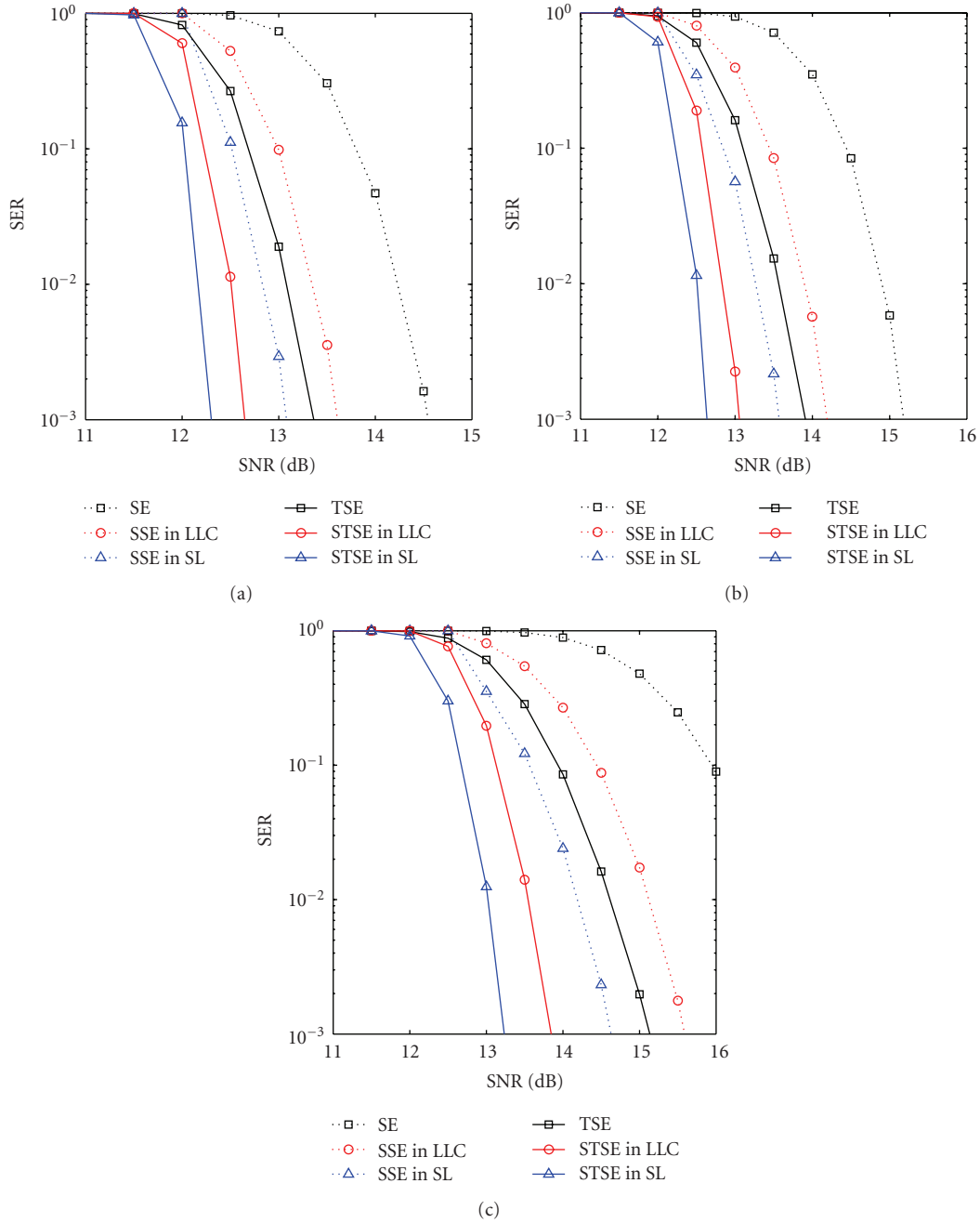


FIGURE 11: The SER simulation results for “WBC over DVB-H”: (a)  $f_D = 10$  Hz; (b)  $f_D = 40$  Hz; (c)  $f_D = 80$  Hz.

The IPER and SER simulation results for SE, SSE, TSE, and STSE are shown in Figures 10 and 11, respectively. The analysis of these results is as follows.

*The Doppler Effect.* As can be seen from the results, IPER/SER worsen when the Doppler frequency increases, especially for the SE scheme. To get IPER/SER below 1% (WBC datacasting requirement), the received signal value should be increased about 0.5–1 dB for TSE schemes and 1.5–2.5 dB for SE schemes for  $f_D = 80$  Hz comparing with  $f_D = 10$  Hz.

*The Section-Based and TS-Based Effect.* As the TS packet is smaller than the IP packet, a byte error in a TS packet will not mark the corresponding IP packet in error; thus the performance of TSE and STSE is better than SE and SSE. The results show that IPER/SER of the TS-based algorithms can gain 1-2 dB comparing with the section-based algorithms.

*The Smart Cross-Layer Decoding Effect at the Link Layer.* At the link layer, an ADP PED scheme is used on SE/TSE to improve reliability. The results show that, to get IPER/SER below 1%, the SSE/STSE gain is about 0.6-1 dB comparing

with SE/TSE when  $f_D = 10$  Hz, and about 1-2 dB when  $f_D = 80$  Hz. The results also show that in order to get IPER/SER below 1%, the new STSE scheme can gain 2 dB comparing with SE when  $f_D = 10$  Hz and 3.5 dB when  $f_D = 80$  Hz.

*The Smart Cross-Layer Decoding Effect at the Service Layer.* With the use of the ADP PE+BED decoding scheme, the IPER/SER at the service layer can gain additional 0.5–1 dB comparing with the IPER/SER at the link layer.

## 6. Conclusion

The performance of the “WBC over DVB-H” system can benefit from DVB-H’s time-slicing and multiprotocol encapsulation-forward error correction (MPE-FEC) features. This DVB-H’s IPDC system design facilitates WBCs sharing bandwidth resources with other DVB-H services. This should help smooth the WBC standardization process. It also facilitates further actions to improve error protection of the WBC information, over and above that offered by MPE-FEC which itself is designed for particularly difficult reception situations.

Considering the commercial importance of the WBC services it is likely a high QoS will be required than the presently foreseen IPDC audio and video services. This paper has addressed techniques to improve error protection. Here the development of two novel smart cross-layer coding schemes based on the section erasure decoding and transport stream (TS) erasure decoding has been described. Based on an analysis of the error rate and on simulations using a wireless Rayleigh fading channel with received signal envelope having a central chi-square distribution, an approximation of the performance improvement has been obtained. A two-state packet-level run length model (2SRL) was introduced to evaluate the output statistics of MPEG-2 TS packets in a DVB-H fading environment. The results have confirmed that the newly proposed smart cross-layer decoding schemes can improve the error protection for the “WBC over DVB-H” system, over the MPE-FEC alone.

## Acknowledgment

This publication has been supported by the Irish Research Council for Science, Engineering and Technology (IRCSET) and the Telecommunication Research Centre, University of Limerick, Ireland.

## References

- [1] M. O’Droma and I. Ganchev, “Towards a ubiquitous consumer wireless world,” *IEEE Wireless Communications Magazine*, vol. 14, no. 1, pp. 52–63, 2007.
- [2] P. Flynn, I. Ganchev, and M. O’Droma, “Wireless billboard channels: vehicle and infrastructural support for advertisement, discovery and association of UCWW services,” in *Annual Review of Communications*, Vol. 59, pp. 493–504, International Engineering Consortium, Chicago, Ill, USA, 2006.
- [3] Zh. Ji, I. Ganchev, and M. O’Droma, “Performance evaluation of ‘WBC over DVB-H’ system,” *IEEE Transactions on Consumer Electronics*, vol. 55, no. 2, pp. 754–762, 2009.
- [4] Zh. Ji, I. Ganchev, and M. O’Droma, “Building a ‘WBC over DVB-H’ software testbed,” in *Proceedings of the 13th IEEE International Symposium on Consumer Electronics (ISCE ’09)*, pp. 769–772, Kyoto, Japan, May 2009.
- [5] M. S. O’Droma and I. Ganchev, “Enabling an always best-connected defined 4G wireless world,” in *Annual Review of Communications*, Vol. 57, pp. 1157–1170, International Engineering Consortium, Chicago, Ill, USA, 2004.
- [6] M. O’Droma, I. Ganchev, G. Morabito, et al., “Always best connected enabled 4G wireless world,” in *Proceedings of the 12th IST Summit on Mobile and Wireless Communications*, pp. 710–716, Aveiro, Portugal, June 2003.
- [7] I. Ganchev, M. S. O’Droma, M. Siebert, et al., “A 4G generic ANWIRE system and service integration architecture,” *ACM SIGMOBILE Mobile Computing and Communications Review*, vol. 10, pp. 13–30, 2006.
- [8] ETSI, “Digital Video Broadcasting (DVB); DVB-H Implementation Guidelines,” ETSI TR 102 377, V1.4.1, 2009.
- [9] M. Kornfeld and G. May, “DVB-H and IP datacast—broadcast to handheld devices,” *IEEE Transactions on Broadcasting*, vol. 53, no. 1, pp. 161–170, 2007.
- [10] X. Yang, J. Vare, and T. J. Owens, “A survey of handover algorithms in DVB-H,” *IEEE Communications Surveys & Tutorials*, vol. 8, no. 4, pp. 16–29, 2007.
- [11] Zh. Ji, I. Ganchev, and M. O’Droma, “Efficient collecting, clustering, scheduling, and indexing schemes for advertisement of services over wireless billboard channels,” in *Proceedings of the 15th International Conference on Telecommunications (ICT ’08)*, pp. 225–230, Saint Petersburg, Russia, June 2008.
- [12] J. Paavola, H. Himmanen, T. Jokela, J. Poikonen, and V. Ipatov, “The performance analysis of MPE-FEC decoding methods at the DVB-H link layer for efficient IP packet retrieval,” *IEEE Transactions on Broadcasting*, vol. 53, no. 1, pp. 263–275, 2007.
- [13] H. Joki and J. Paavola, “A novel algorithm for decapsulation and decoding of DVB-H link layer forward error correction,” in *Proceedings of the IEEE International Conference on Communications (ICC ’06)*, vol. 11, pp. 5283–5288, Istanbul, Turkey, June 2006.
- [14] ETSI, EN 300 744, “Digital Video Broadcasting (DVB); Framing Structure, Channel Coding and Modulation for Digital Terrestrial Television,” V1.6.1, January 2009.
- [15] Zh. Ji, I. Ganchev, and M. O’Droma, “Reliable and efficient advertisements delivery protocol for use on wireless billboard channels,” in *Proceedings of 12th IEEE the International Symposium on Consumer Electronics (ISCE ’08)*, pp. 1–4, Algarve, Portugal, April 2008.
- [16] Zh. Ji, I. Ganchev, and M. O’Droma, “‘WBC over DVB-H’ testbed design, development and results,” *EURASIP Journal on Wireless Communications and Networking*, vol. 2010, Article ID 769683, 18 pages, 2010.
- [17] G. Klyne, F. Reynolds, C. Woodrow, et al., “Composite Capability/Preference Profiles (CC/PP): Structure and Vocabularies,” W3C Recommendation, 2004, <http://www.w3.org/TR/CCPP-struct-vocab/>.
- [18] P. Dent, G. E. Bottomley, and T. Croft, “Jakes fading model revisited,” *Electronics Letters*, vol. 29, no. 13, pp. 1162–1163, 1993.
- [19] E. N. Gilbert, “Capacity of a burst-noise channel,” *The Bell System Technical Journal*, vol. 39, pp. 1253–1265, 1960.
- [20] C. Xiao, Y. R. Zheng, and N. C. Beaulieu, “Novel sum-of-sinusoids simulation models for rayleigh and rician fading

- channels," *IEEE Transactions on Wireless Communications*, vol. 5, no. 12, pp. 3667–3678, 2006.
- [21] Q. Zhang and S. A. Kassam, "Finite-state markov model for rayleigh fading channels," *IEEE Transactions on Communications*, vol. 47, no. 11, pp. 1688–1692, 1999.
- [22] J. McDougall and S. Miller, "Sensitivity of wireless network simulations to a two-state Markov model channel approximation," in *Proceedings of the IEEE Global Telecommunications Conference (GLOBECOM '03)*, vol. 2, pp. 697–701, San Francisco, Calif, USA, December 2003.
- [23] J. G. Proakis, *Digital Communications*, McGraw-Hill, New York, NY, USA, 4th edition, 2001.
- [24] A. Goldsmith, *Wireless Communications*, Cambridge University Press, Cambridge, UK, 2005.
- [25] X. Dong and N. C. Beaulieu, "Average level crossing rate and average fade duration of low-order maximal ratio diversity with unbalanced channels," *IEEE Communications Letters*, vol. 6, no. 4, pp. 135–137, 2002.